

## Spatial distribution and structure of remotely sensed surface water content estimated by a thermal inertia approach

ANTONIO COPPOLA<sup>1</sup>, ANGELO BASILE<sup>2</sup>,  
MASSIMO MENENTI<sup>2</sup>, MAURIZIO BUONANNO<sup>2</sup>,  
JEROME COLIN<sup>3</sup>, ROBERTO DE MASCELLIS<sup>2</sup>,  
MARCO ESPOSITO<sup>2</sup>, UGO LAZZARO<sup>2</sup>,  
VINCENZO MAGLIULO<sup>2</sup> & PIERO MANNA<sup>4</sup>

<sup>1</sup> Department for Agro-Forestry Systems Management, Hydraulics Division,  
University of Basilicata, Potenza, Italy  
[antonio.coppola@unibas.it](mailto:antonio.coppola@unibas.it)

<sup>2</sup> Institute for Mediterranean Agricultural and Forestry Systems (ISAFoM),  
National Research Council (CNR), Ercolano (NA), Italy

<sup>3</sup> Laboratoire des Sciences de l'Image, de l'Informatique et de la Télédétection, (CNRS/ULP),  
Strasbourg, France

<sup>4</sup> Department of Soil Science, Plant and Environment (DISSPA), University of Napoli "Federico II", Portici, NA, Italy

**Abstract** A major problem recurring in soil and hydrological sciences is the representation of flow and transport processes in the presence of large spatial and temporal variability of soil hydraulic properties. Their measurement is normally time consuming and expensive and it is usually considered impractical to perform sufficiently dense *in situ* measurements. Measurement techniques primarily designed for field, plot or local scale monitoring, are often impractical for larger scales such as watersheds. However, remote sensing from air- or space-borne platforms offers the possibility to address this problem by providing large spatial coverage and temporal continuity. A crucial variable that can actually be monitored by remote sensors is the water content in a thin soil layer, usually up to a depth of 5 cm below the surface. However, difficulties arise in the estimation of the vertical and horizontal distribution of the water content within the soil profile, which are closely connected to soil hydraulic properties and their spatial distribution. A promising approach for estimating soil water content profiles is the integration of remote sensing of surface water content and hydrological modelling. A major goal of the scientific group is to develop a practical and robust procedure for estimating water contents throughout the soil profile from surface water contents to be deduced from thermal inertia data, which in turn have to be estimated by multi-spectral remote sensing data. The procedure is largely based on the integration of the remote sensing information into a hydrological model to be used in a stochastic simulation framework, in the perspective of predicting the crucial vadose zone processes at large scale. As a first step, in this work we will show some preliminary results from aircraft image analyses and their validation by field campaign data. The data extracted from the airborne sensors provided the opportunity to retrieve land surface temperatures with a very high spatial resolution. The distribution of surface moisture, as deduced by the thermal inertia estimates, was compared to the surface water content maps measured *in situ* by TDR-based probes.

**Key words** remote sensing; soil spatial variability; soil thermal inertia; soil water content

## INTRODUCTION

A major objective for Earth scientists throughout the world is to develop a practical procedure for estimating the water content near the soil surface and throughout the root zone or in the top metre, from remotely sensed data. Indeed, soil water status in the root zone over large areas provides important input for many agricultural and hydrological applications. Given the central role of soil water content in land surface processes, its spatio-temporal status and trends should be assessed at multiple scales to serve as an effective tool for strategic management and protection of water resources.

However, soil water content measurement over large areas is a complex task and no large-area networks exist to measure soil water content at the high frequency, multiple depths and fine spatial resolution that is required for various applications. The complexity of the issue is largely a consequence of the spatial heterogeneity of the vadose zone, through which land surface, groundwater and atmosphere interact for the exchange of energy and mass (water, solutes and gases).

While conventional methods (e.g. TDR) are suitable for local-scale or field plot monitoring (Comegna *et al.*, 1999; Basile *et al.*, 2003, 2006), they are not feasible for the watershed or regional scale. Remote sensing of soil water content from air- or space-borne platforms would offer the possibility to partially overcome this problem as it provides the large spatial coverage and temporal continuity necessary for many applications (Menenti 1984; Menenti & Choudhury, 1993; Jackson *et al.*, 1999). A crucial variable that can actually be monitored by remote sensors is the water content in a thin soil layer, usually up to a depth of 0.05 m below the soil surface (Jackson & Schmugge, 1989). To the contrary, difficulties arise in the estimation of the water content storage along the soil profile and its spatial (horizontal) distribution, which are closely connected to soil hydraulic properties and their spatial distribution.

Alternatively, many reliable hydrological models are available for calculating soil water content along the whole soil profile. For large scale studies concerned with large areas that may exhibit high spatial (and temporal) variability, while searching for reliable soil water content predictions one invariably faces difficulties finding adequate data sets of soil hydraulic properties, the measurement of which is normally time consuming and expensive.

It has been suggested (Kostov & Jackson, 1993; Ragab, 1995; Wey, 1995) that the best operational soil water content estimates might be obtained by integrating remote-sensing data and computational modelling. A range of possible strategies includes data assimilation and model calibration and are outlined below. A synthesis of data assimilation and inversion approaches has been provided by Entekhabi *et al.* (1994), who presented a theoretical methodology for solving the inverse problem for soil water content using sequential assimilation of remotely sensed surface data.

While searching for the best method to assimilate surface water contents, one invariably faces difficulties finding adequate data sets of hydraulic properties measurements to be used as input in the hydrological models. For large-scale studies concerned with large areas that may exhibit complex spatial (and temporal) variability of soil hydraulic properties, it is usually considered impractical to perform a sufficient number of direct measurements. Realistically, dealing with such complexity involves an approach that takes into account a stochastic component of the variability. In the

stochastic approach, the hydraulic parameters are treated as spatial random functions whose mean and covariance functions completely characterize spatial variability and the spatial structure of the hydraulic properties.

With such premises, the main objective of this research group is to develop a deterministic/stochastic methodology aimed at characterizing the large-scale spatial structure of the hydraulic properties by integrating a soil-water model based on the Richard's equation, used in stochastic context, with surface water content maps from airborne sensors. The latter will be deduced from thermal inertia data, which in turn must be estimated by thermal infrared remote sensing. The final aim is to develop a practical and robust procedure for estimating the spatial variability of hydraulic properties, through which the water contents throughout the soil profile can be easily computed.

As a first step, we will show some preliminary results from aircraft images analysis and their validation by field campaigns data in this paper. The data extracted from the airborne sensors provided the opportunity of retrieving land surface temperatures with a very high spatial resolution. The surface water content pattern, as deduced by the thermal inertia estimations, was compared to the surface water content maps measured *in situ* by time domain reflectometry-based probes.

## **MATERIAL AND METHODS**

### **The experimental site**

The experiment was performed at the IMPROSTA experimental farm, located in the Sele valley at 20 m a.s.l., 40°33'24"N and 14°58'30"E, in Eboli (SA), south of Italy. The soil is a clay loam developed on alluvial plain and classified as Inceptisol with vertic characteristics.

### **Ground measurements**

The soil water content was measured by means of Time Domain Reflectometry (Robinson *et al.*, 2003). We used three 1502 C Tektronix cable testers (Tektronix, Beaverton, Oregon, USA) with three-rod probes (rods length, diameter and spacing were 65, 3 and 17 mm, respectively) vertically inserted at the soil surface. The measurements, performed in between the air flights, took approximately 1 hour.

The ground measurements were performed on the 29 September 2006 in 105 points of a regular grid (20 m × 20 m) on 3.5 ha bare soil after a corn crop harvesting. The sampling grid was established with a metric tape and a tilting level with telescope. The absolute position of the grid was measured at about 2 m horizontal accuracy by surveying points in the first and the last row using a *Magellan Promark 2* GPS with external antenna. After the measurements, undisturbed and bulk soil samples were collected at a depth of 0–7 cm, to determine bulk density (core method) and clay content (hydrometer method), respectively (Dane & Topp, 2002).

## Remote sensor measurements

Remote sensing data were collected using a *FLIR A40M* thermal infrared camera and a *Geospatial Systems* (previously *DuncanTech*) *MS4100 CIR* multispectral camera.

*FLIR A40M* thermal infrared camera is a FLIR long wave, Focal Plane Array camera capable of temperature measurement. It is based on “bolometer” technology, and allows the measurement of the electromagnetic radiation relative at the spectrum from 7500–13 000 nm.

*Geospatial Systems MS4100 CIR* is a 3-CCDs progressive-scan digital camera with a resolution of  $1920 \times 1080$  pixels at a rate of 10 frames per second. Its 3-CCDs detect in Near Infrared (700–900 nm), Red (600–700 nm) and Green (500–600 nm), respectively.

Both cameras have been radiometrically calibrated to be used for quantitative measurements. Particularly, in a room completely darkened, the VNIR camera was calibrated with respect to the radiance measured by the FieldSpec FR leaving a Spectralon panel (a near 100% diffuse (Lambertian) reference reflectance panel) illuminated by two lamps with regulated intensity.

The aerial survey was carried out by mounting the cameras on a *Sky Arrow 650 TCNS ERA* light aircraft (Fig. 1). It is a tandem seat aircraft equipped by NOAA with the Mobile Flux Platform (MFP) which consists of a set of sensors for atmospheric measurements.

During the survey MFP’s sensors collected the following environmental variables: wind direction and intensity, air temperature, air humidity, CO<sub>2</sub> and H<sub>2</sub>O concentration in the free atmosphere, net radiation level and Photosynthetically Active Radiation. Some of these data have been used for image atmospheric correction.

The aerial survey consisted of two flights taken in the same day of ground sampling, the first one early in the morning, and the second around noon, approximately at the daily lower and higher temperature.

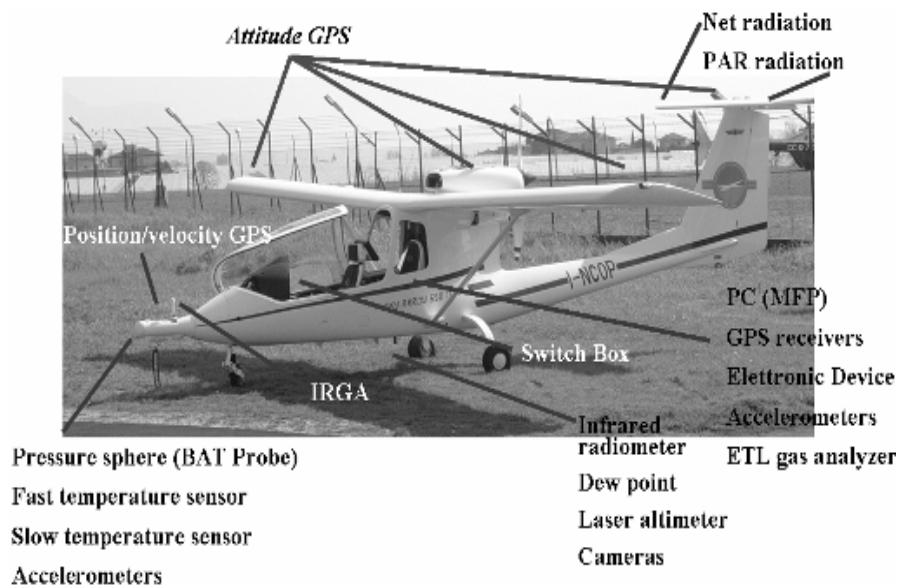


**Fig. 1** *Sky Arrow 650 TCNS ERA* light aircraft and sensors location.

At the chosen flight height above ground (773 m) image ground resolution for *FLIR A40M* and *Geospatial Systems MS4100* CIR was 2 m and 0.4 m, respectively.

After collection, images were geometrically registered for allowing cross-analysis. Derived data was finally georeferenced using the 1:5000 nominal scale vector map to be able to integrate remote sensed and field data.

## THEORY

Numerous researchers have shown that near-surface soil moisture content can be estimated by thermal infra-red remote sensing. Thermal infra-red remote sensing operates in the 3–14  $\mu\text{m}$  wavelength region of the electromagnetic spectrum and measures the thermal emission of the Earth. Methods for inferring near-surface soil moisture content using thermal infra-red remote sensors rely upon using the thermal infra-red data to measure the soil surface temperature, as soil moisture influences the thermal properties of the soil. To recover the surface temperature from at-sensor brightness temperature, it is necessary to estimate both surface emissivity and the effects of the atmosphere on the measured radiance. Surface emissivity can be either locally estimated or mapped from remotely sensed images using methods of various complexity (Van de Griend & Owe, 1993; Li *et al.*, 1999). At-sensor radiance must also be corrected from the effects of the atmosphere, i.e. spectral transmittance and path radiance. These corrections are carried out using atmospheric profile data and a radiative transfer code like MODTRAN4.

As soil moisture content has a strong influence on the thermal properties of the Earth's surface, relatively minor changes in moisture content have a large effect on the bulk thermal properties of the ground. Thus, areas having higher soil moisture content are cooler during the day and warmer at night, everything else being constant.

The amplitude of the diurnal range of soil surface temperature is a function of soil thermal properties, soil–vegetation albedo, vegetation structure (magnitude of soil heat flux relative to net radiation; roughness in relation with heat exchanges), and meteorological variables (solar radiation, air temperature, cloudiness, wind, aerosol concentration, etc.). Soil thermal properties are the soil thermal conductivity  $\lambda$  ( $\text{W m}^{-1} \text{K}^{-1}$ ) and the soil heat capacity  $C^*$  ( $\text{J kg}^{-1} \text{K}^{-1}$ ) through which the soil thermal inertia can be defined:

$$P = (\lambda \rho_b C^*)^{1/2} [\text{J m}^{-2} \text{K}^{-1} \text{s}^{-1/2}] \quad (1)$$

where  $\rho_b$  ( $\text{kg m}^{-3}$ ) is the soil bulk density.

Day–night temperature differences may be used to infer thermal inertia and thus soil water content. Indeed, the difference between day and night surface temperatures is a function of the thermal inertia of the system, which is controlled by the amount of water in the soil. For a given soil in a wet phase, the diurnal temperature range will be smaller than for the same soil when dry. The amplitude of the diurnal range of soil surface temperature has been found to have a good correlation with the soil moisture content in the 0 to 4 cm layers of the soil (Schmugge *et al.*, 1980).

The thermal inertia can be calculated according to Idso (1976) and Menenti (1984). For a sinusoidal varying surface heat flux of amplitude  $\Delta G/2$ , the variation in the surface temperature around some mean value  $T_{s,av}$  is given by:

$$(T_s - T_{s,av}) = \frac{\Delta G/2 \cdot \sin(\omega t - 1/4\pi)}{\sqrt{\omega \lambda \rho_b C^*}} \Rightarrow 0.5 \cdot \Delta T_s = \frac{\Delta G}{P\sqrt{\omega}} \quad (2)$$

where  $\omega$  is the frequency corresponding to a 24 h period ( $\omega = 2\pi/86\,400 \text{ s}^{-1}$ ) and  $\Delta T_s$  is the difference between the maximum and minimum surface temperature. This way, the thermal inertia can be calculated once both day–night temperature and surface heat flux differences are available.

The soil heat flux can be obtained by fitting net radiation with fractional vegetation cover:

$$G = Rn \cdot [\Gamma_c + (1 - f_c) \cdot (\Gamma_s - \Gamma_c)] \quad (3)$$

where  $\Gamma_c = 0.05$  and  $\Gamma_s = 0.315$  being the ratio of  $G/Rn$  for full vegetated surface and bare soil, respectively (Kustas & Daughtry, 1989; Monteith & Unsworth, 1990).

Net radiation  $Rn$  is calculated as follow:

$$Rn = Glo \cdot (1 - \alpha) + R_{ATM\downarrow} - (1 - \varepsilon_s) \cdot R_{ATM\downarrow} - \varepsilon_s \sigma T_s^4 \quad (4)$$

where  $Glo$  is the global radiation measured at ground level on site,  $\alpha$  the albedo calculated from the VNIR image following a calibration curve of albedo vs reflectance obtained using ASTER spectral library,  $R_{ATM\downarrow}$  the incoming IR radiation estimated from the atmospheric radiosounding data using the radiative transfer code MODTRAN4, and  $\varepsilon_s$  the surface emissivity derived from NDVI following:

$$\varepsilon_s = a + b - \ln(\text{NDVI}) \quad (5)$$

with  $a = 1.009$  and  $b = 0.047$ , Van de Griend & Owe (1993).

Thermal inertia-based surface water contents maps can be estimated by using empirical relationships among volumetric water content,  $\theta_v$ , volumetric heat capacity,  $C^*$ , and thermal conductivity,  $\lambda$ , once the clay mass fraction,  $m_c$ , and  $\rho_b$  are known. Herein the procedure proposed by Campbell (1985) is adopted, according to the following equations:

$$C^* = c_s + c_w \frac{\theta_v}{\rho_b} \quad (6)$$

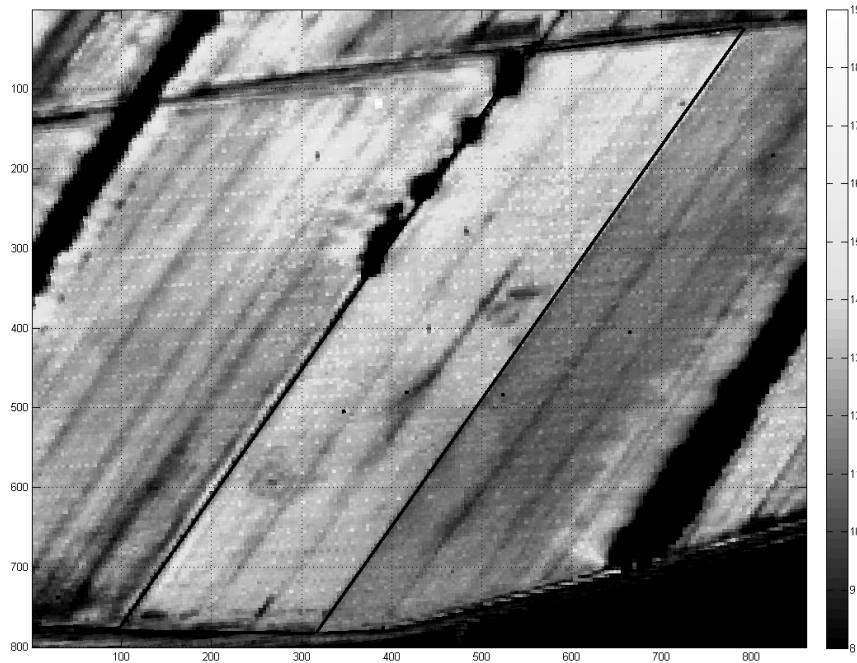
with  $c_s$  and  $c_w$  the average specific heat of the solid constituents and the specific heat of water, respectively.

$$\begin{aligned} \lambda &= A + B\theta_v - (A - D)\exp(-C\theta_v)^E \\ A &= 0.65 - 0.78\rho_b + 0.60\rho_b^2 \\ B &= 1.06\rho_b \\ C &= 1 + \left( \frac{2.6}{m_c^{1/2}} \right) \\ D &= 0.03 + 0.1\rho_b^2 \end{aligned} \quad (7)$$

Thus, the volumetric water content may be estimated by replacing equations (6) and (7) in the equation (1), calculating  $P$  according to equations (2–5), and solving (inverting) for  $\theta_v$ .

## RESULTS AND DISCUSSION

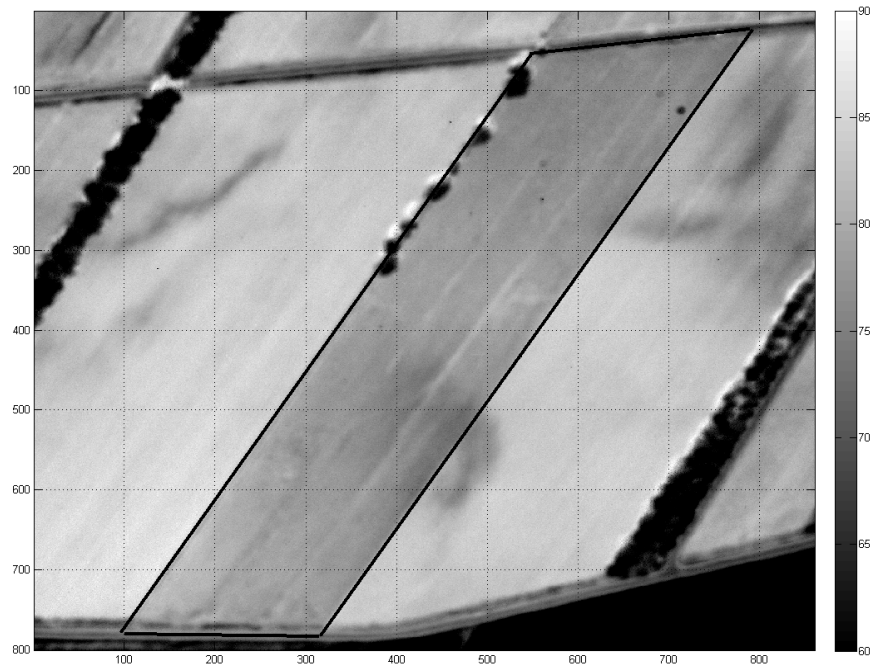
In Fig. 2 the difference in surface temperature measured by the *FLIR A40M* thermal infrared camera at early morning and noon are shown. The area inside the black frame is the experimental site.



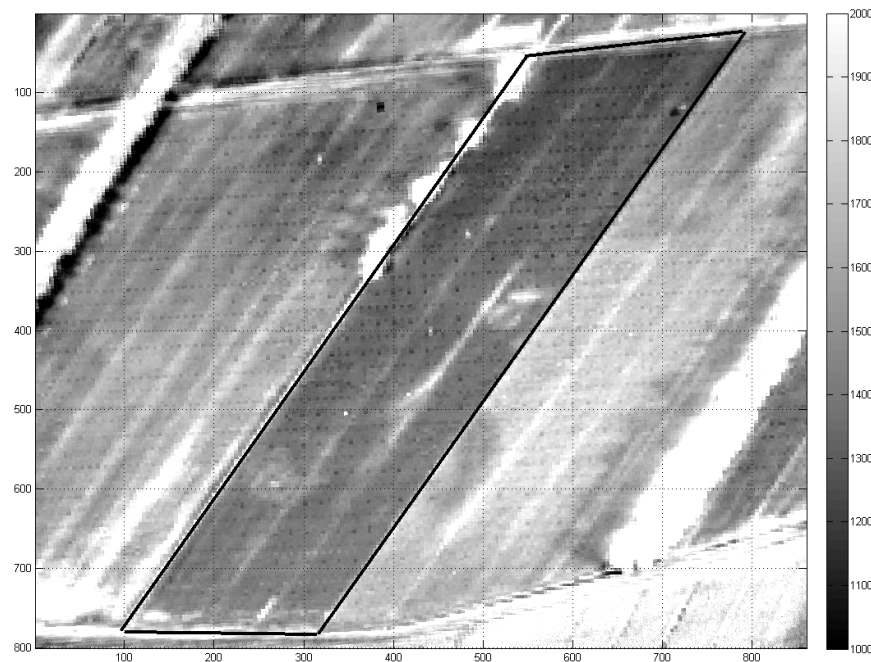
**Fig. 2** Temperature difference between early morning and afternoon (K).

Figure 3 shows the map of the difference of the soil heat flux determined by the procedure reported in the Theory section. Values of soil heat flux vary from  $25 \text{ W m}^{-2}$  in the morning to  $75 \text{ W m}^{-2}$  at noon over surfaces fully covered by vegetation, whereas values over bare soil vary from  $60 \text{ W m}^{-2}$  in the morning to  $145 \text{ W m}^{-2}$  at noon. The largest variations can be found close to tree bands, for pixels shadowed at 07:00 h, and exposed to the sun during the morning.

In Fig. 4 the thermal inertia map derived from aircraft measurements is shown. The amplitude of the fluctuations in surface temperature over the IMPROSTA experimental field is inversely proportional to the thermal inertia values (Figs 2 and 4). In the northern part of the field, larger temperature fluctuations (up to 15 K) and smaller thermal inertia values ( $\sim 1200 \text{ J m}^{-2} \text{ K}^{-1} \text{ s}^{-1/2}$ ) are present. Conversely, the southern part shows smaller temperature fluctuations ( $\sim 12 \text{ K}$ ) and larger thermal inertia values ( $\sim 1500 \text{ J m}^{-2} \text{ K}^{-1} \text{ s}^{-1/2}$ ).



**Fig. 3** Differences of soil heat flux between morning and afternoon ( $\text{W m}^{-2}$ )



**Fig. 4** Thermal inertia evaluated from remote sensed images ( $\text{J m}^{-2} \text{K}^{-1} \text{s}^{-1/2}$ )

The measured soil water contents,  $\theta_{meas}$ , show a mean and standard deviation values of 0.165 and 0.025 ( $\text{cm}^3 \text{cm}^{-3}$ ), respectively. Such values indicate a relatively small variability, though the investigated field contain at least three different soil units identified on a 1:5000 scale soil map. This could be ascribed to a relatively homogeneity induced by the intensive cultivations and tillage.



Figure 5(a) shows the TDR water content map from TDR measurements obtained by an ordinary kriging algorithm (Journel & Huijbregts, 1978). Notwithstanding

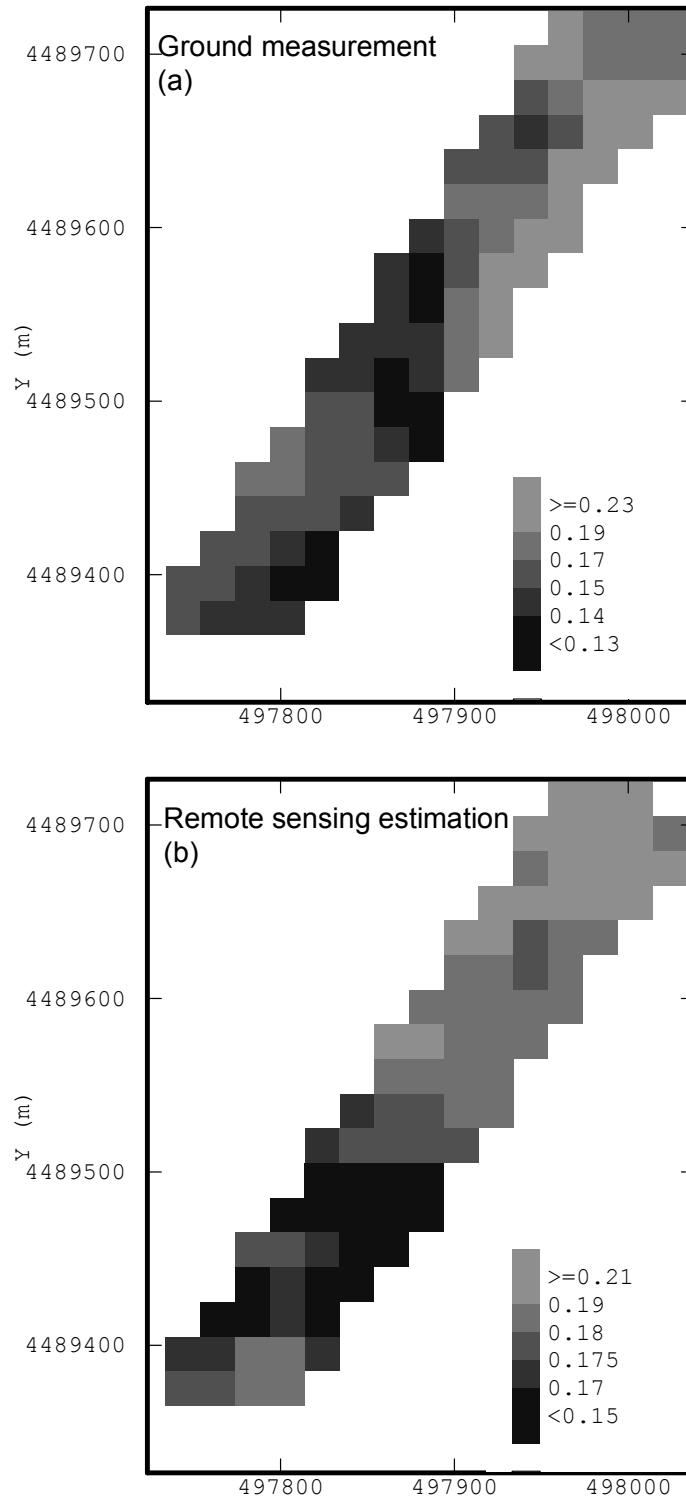


**Fig. 5** Map of soil water content measured at ground level by TDR (a) and estimated from remote sensing data by the thermal inertia approach (b).

the small variation range, some spatial pattern can be identified. In fact, wetter and drier areas can be roughly distinguished in the northern and southern part of the field, respectively, and a relatively homogeneous behaviour can be recognized in each of these two areas.

A clear spatial structure can also be identified by observing the corresponding isotropic spherical variogram (Fig. 6(a)), having sill and range of 0.0006 and 73 m, respectively, with a small nugget effect. The range is the distance over which pairs of data are spatially correlated, while the sill is the variogram variance. The dashed line

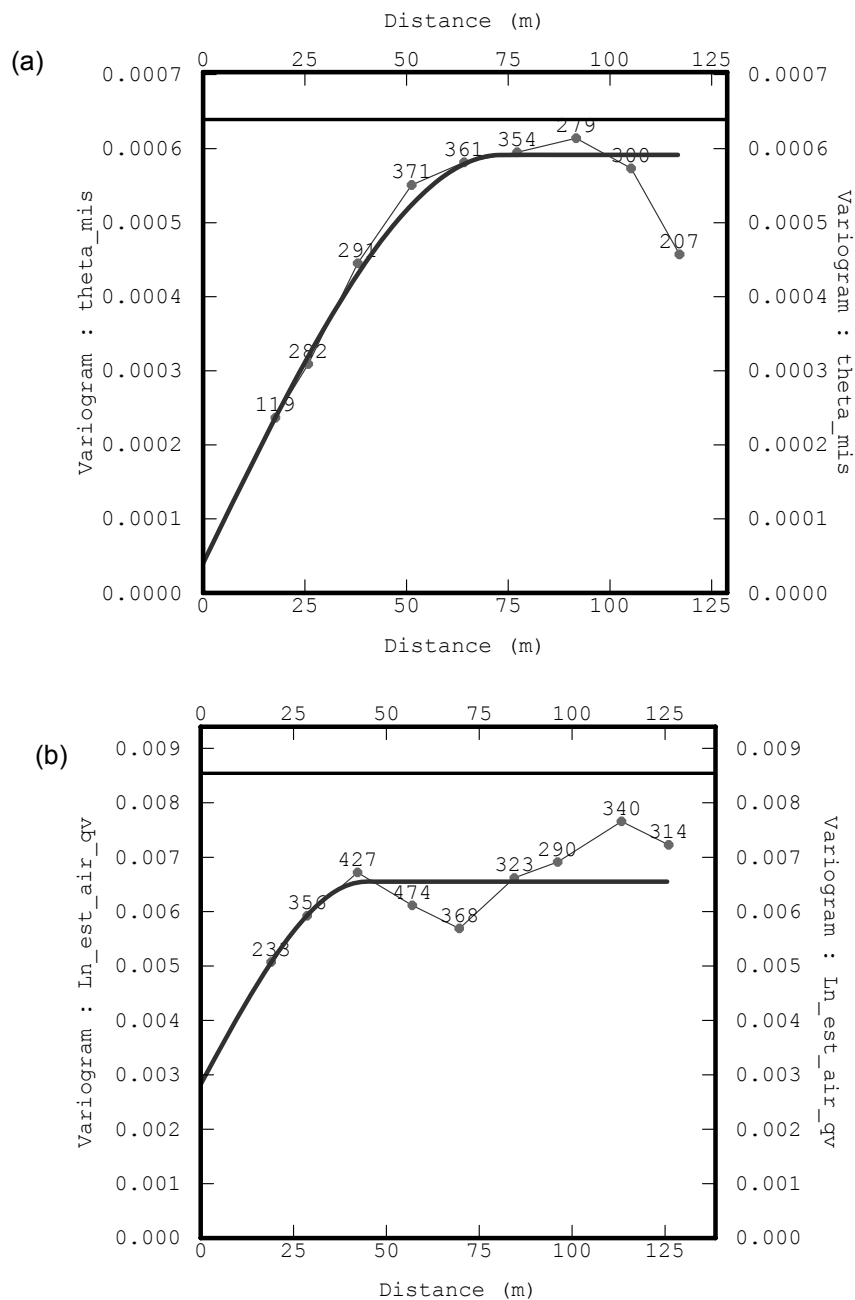


**Fig. 6** Variograms of soil water content measured at ground level by TDR (a) and estimated from remote sensing data by the thermal inertia approach (b).

represents the value of the experimental variance. The nugget effect is a discontinuity at the origin of the variogram and relates to measurement errors and to spatial sources of variations at distances smaller than the shortest sampling interval (Journel & Huijbregts, 1978).

In order to properly compare the maps of soil water contents derived from different sensor resolution, the variable should have the same support size. Therefore, the map of thermal inertia (Fig. 3), prior to being transformed into a map of soil water content according to equations (6–7), has been up-scaled to a grid resolution of about  $20 \times 20$  m by averaging the original pixel values.

The  $20 \times 20$  m averaged estimation of water content from airborne measurement, shows a mean of about  $0.181 \text{ (cm}^3 \text{ cm}^{-3}\text{)}$  with a standard deviation of  $0.019 \text{ (cm}^3 \text{ cm}^{-3}\text{)}$ . Both values are very close to those coming from the ground measurements. This is the first positive outcome, indicative of the method's capability to both infer the average and variability in water content estimation.

Looking at the spatial variability of the estimated data, Fig. 6(a) shows the experimental and the fitted isotropic spherical variogram of the natural logarithm water content estimated from remote data. The data were transformed to the natural logarithm because they have a slight log-normal distribution (data not shown). The variogram shows a consistent nugget effect of about 50% of the variogram variance and a range of about 45 m

The two measurement procedures roughly determine the same patterns of variability. Higher water contents are on the northern part of the experimental field. The measured soil water content shows also variability with increasing values along the E–W direction. The same pattern was difficult to distinguish in the data from the remote (Fig. 5(b)), probably due to the re-sampling procedure of the thermal inertia data, from 0.40 to 20 m of resolution.

## CONCLUSIONS

The proposed procedure allows the estimation of integrated soil water content up to a depth of about 7 cm. Daily maximum differences of temperature and soil heat flux estimated from remote data are the key information to achieve the thermal inertia. Moreover, ground estimation of soil thermal conductivity and soil heat capacity from basic soil information (mainly bulk density and clay content) allows the inference of soil water content values.

The estimated soil water content values were compared with those measured at ground level by the TDR technique. In summary, the results of this comparison between measured and estimated were promising because: (1) the very close average ( $0.165$  vs  $0.181 \text{ cm}^3 \text{ cm}^{-3}$ ) and standard deviation ( $0.025$  vs  $0.019 \text{ cm}^3 \text{ cm}^{-3}$ ); (2) the similar range of the experimental variograms (73 vs 45 m); and (3) the recognized similar pattern of variability despite the very low variability shown by the data, both measured and estimated.

**Acknowledgements** This study was funded by the SeSIRCA Regione Campania in the framework of the Project “Agricultural nitrate vulnerability in Campania Region – Programma Interregionale “Agricoltura e Qualità – Misura 5”

## REFERENCES

- Basile, A., Ciollaro, G. & Coppola, A. (2003) Hysteresis in soil-water characteristics as a key to interpreting comparisons of laboratory and field measured hydraulic properties. *Water Resour. Res.* **39**(12), 1355.
- Basile, A., Coppola, A., De Mascellis, R. & Randazzo, L. (2006) A hysteresis based scaling approach to deduce field hydraulic behaviour from core scale measurements. *Vadose Zone J.* **5**, 1005–1016.
- Campbell, G. S. (1985) *Soil Physics with BASIC-Transport Models for Soil-Plant Systems*. Elsevier, New York, USA.
- Comegna, V., Coppola, A. & Sommella A. (1999) Nonreactive solute transport in variously structured soil materials as determined by laboratory-based time domain reflectometry (TDR). *Geoderma* **92**, 167–184.
- Dane, J. H. & Topp, G. C. (2002) *Methods of soil analysis*. SSSA Book Ser. 5. SSSA, Madison, Wisconsin, USA.
- Entekhabi, D., Nakamura, H. & Njoku, E. G. (1994) Solving the inverse problem for soil moisture and temperature profiles by sequential assimilation of multifrequency remotely sensed observations. *IEEE Trans. Geosci. Remote Sens.* **32**:438–448.
- Idso, S. B., Jackson, R. D. & Reginato, R. J. (1976) Compensating for environmental variability in the thermal inertia approach to remote sensing of soil moisture. *J. Appl. Meteorol.* **15**, 811–817.
- Jackson, T. J. & Schmugge, T. J. (1989) Passive microwave remote sensing system for soil moisture: some supporting research. *IEEE Trans. Geosci. Remote Sens.* **27**, 225–235.
- Jackson, T. J., Le Vine, D. M. Hsu, A. Y. Oldak, A., Starks, P. J., Swift, C. T. Isham, J. D. & Hakan, M. (1999) Soil moisture mapping at regional scales using microwave radiometry: The Southern Great Plains hydrology experiment. *IEEE Trans. Geosci. Remote Sens.* **37**, 2136–2151.
- Journel, A. G. & Huijbregts, C. J. (1978) *Mining Geostatistics*. Academic, San Diego, California, USA.
- Kostov, K. G. & Jackson, T. J. (1993) Estimating profile soil moisture from surface layer measurements—a review. In: *Proc. The International Society for Optical Engineering*, vol. 1941 (Orlando, Florida), 125–136.
- Li, Z. -L., Becker, F., Stoll, M. -P. & Wan, Z. (1999) Evaluation of six methods for extracting relative emissivity spectra from thermal infrared images. *Remote Sens. Environ.* **69**, 197–214.
- Kustas, W. P. & Daughtry, C. S. T. (1989) Estimation of the soil heat flux / net radiation ratio from spectral data. *Agric. For. Meteorol.* **49**, 205–223.
- Menenti, M. (1984) Physical aspects of and determination of evaporation in deserts applying remote sensing techniques. Report 10 (special issue), Institute for Land and Water Management Research (ICW), The Netherlands.
- Menenti, M. & Choudhury, B. J. (1993) Parametrization of land surface evapotranspiration using a location-dependent potential evapotranspiration and surface temperature range. In: *Exchange Processes at the Land Surface for a Range of Space and Time Scales* (ed. by H. J. Bolle, R. A. Feddes & J. D. Kalma), 561–568. IAHS Publ. 212. IAHS Press, Wallingford, UK.
- Monteith, J. L. & Unsworth, M. H. (1990) *Principles of Environmental Physics*. Edward Arnold Press.
- Ragab, R. (1995) Towards a continuous operational system to estimate the root-zone soil moisture from intermittent remotely sensed surface moisture. *J. Hydrol.* **173**, 1–25.
- Robinson, D. A., Jones, S. B., Wraith, J. M., Or, D. & Friedman, S. P. (2003) A review of advances in dielectric and electrical conductivity measurement in soil using time domain reflectometry. *Vadose Zone J.* **2**, 444–475.
- Schmugge, T. J., Jackson, T. J. & McKim, H. L. (1980) Survey of methods for soil moisture determination. *Water Resour. Res.* **16**(6), 961–979.
- Van de Griend, A. A. & Owe, M. (1993) On the relationship between thermal emissivity and the normalized difference vegetation index for natural surfaces. *Int. J. Remote Sens.* **14**(6), 1119–1131.
- Wei, M. Y. (1995) Soil moisture: Report of a workshop held in Tiburon, California, 25–27 January 1994, NASA Conf. Publ., CP-3319.